Electroluminescence from a Mixed Red–Green–Blue Colloidal Quantum Dot Monolayer

Polina O. Anikeeva,[†,‡] Jonathan E. Halpert,[†,§] Moungi G. Bawendi,*,[§] and Vladimir Bulović[‡]

Laboratory of Organic Optics and Electronics, Department of Electrical Engineering and Computer Science, Massachusetts Institute of Technology, Cambridge, Massachusetts 02139, and Department of Chemistry, Massachusetts Institute of Technology, Cambridge, Massachusetts 02139

ABSTRACT

We demonstrate light emitting devices (LEDs) with a broad spectral emission generated by electroluminescence from a mixed-monolayer of red, green, and blue emitting colloidal quantum dots (QDs) in a hybrid organic/inorganic structure. The colloidal QDs are reproducibly synthesized and yield high luminescence efficiency materials suitable for LED applications. Independent processing of the organic charge transport layers and the QD luminescent layer allows for precise tuning of the emission spectrum without changing the device structure, simply by changing the ratio of different color QDs in the active layer. Spectral tuning is demonstrated through fabrication of white QD-LEDs that exhibit external quantum efficiencies of 0.36% (Commission Internationale de l'Eclairage) coordinates of (0.35, 0.41) at video brightness, and color rendering index of 86 as compared to a 5500 K blackbody reference.

The high luminescence efficiency and the narrow spectral emission of colloidally synthesized quantum dots (QDs)[1] enabled their use in light emitting devices (LEDs)[2,3] to fabricate planar light sources of high color saturation. In this report we demonstrate that by combining multiple QD lumophores in a diode junction device, an arbitrarily broad electroluminescence spectrum can also be generated, with precisely controlled relative intensities of the constituent spectral components.

Previous reports on efficient monochrome QD-LEDs utilized QD lumophores embedded in organic semiconductor charge transport layers to generate saturated color red, green, and blue (RGB) QD-LEDs with peak efficiencies of 2.0%, 0.5%, and 0.2%, respectively.[2–6] Monochrome QD-LEDs with lower efficiencies have also been fabricated using inorganic transport layers, which replaced some of the environmentally sensitive organic films.[7,8] For white color generation, QD lumophores were utilized as a replacement for red[9,10] or green[11] color components in white-light LEDs employing organic emitters. A broad spectral emission using a mixture of QDs has also been demonstrated using red, green, and blue emitting dots embedded in poly(lauryl methacrylate)[12] with a blue GaN or Hg vapor lamp for

excitation. White light photoluminescence from QDs was also obtained by Bowers et al.[13] and Chen et al.[14] in devices in which deep trap QD luminescence was photoexcited by an external ultraviolet LED. However, deep trap emitters, generally defective CdS or ZnSe QDs, are only weakly luminescent, and the defect trap states on QD lumophores are poorly characterized and not easily reproducible from one synthesis to the next. Using three types of QDs as emitters in an electrically driven structure has been previously reported as preliminary work in our group,[15] and as a parallel effort by Li et al.[16] but with efficiencies of more than a factor of 4 lower.

The goal of the present work is to demonstrate reproducible and efficient spectrally broad electroluminescent QD-LEDs with spectral emission tunable across the CIE (Commission Internationale de l'Eclairage) color space. We demonstrate that the electroluminescence spectrum can be precisely tuned in diode junction devices in which the mixed color electroluminescence is derived from a single QD monolayer containing QDs of multiple colors. To demonstrate spectral tunability, we adjust the relative concentrations of QD components in the QD monolayer to obtain white light emitting QD-LEDs with a high color rendering index.

Our devices consist of an indium tin oxide (ITO) anode on top of a glass substrate with a layer of conducting polymer poly(3,4-ethylenedioxythiophene):poly(styrenesulfonate) PE-DOT:PSS as the hole injection layer, a 40 nm thick hole

---

† These authors contributed equally to this work.
‡ Laboratory of Organic Optics and Electronics, Department of Electrical Engineering and Computer Science.
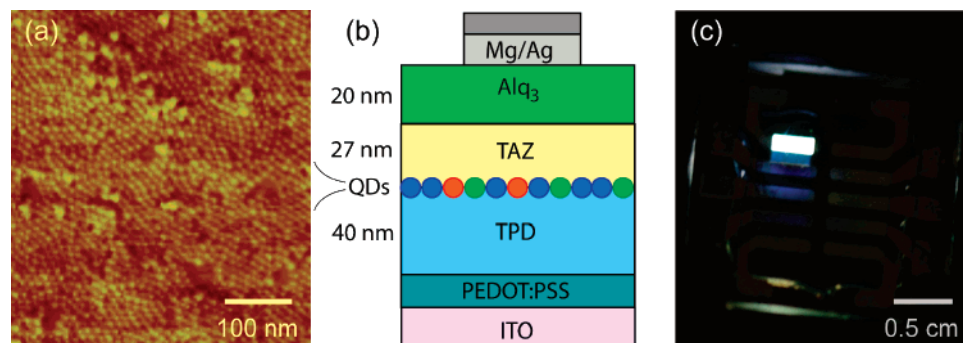§ Department of Chemistry.

Figure 1. (a) Atomic force microscope phase image of blue QDs forming approximately 1.1 monolayers on top of a 40 nm thick TPD film. (b) Device cross section of a white QD-LED. (c) Photograph of a white QD-LED in operation with 10 V of applied forward bias.

transporting layer of *N,N′*-bis(3-methylphenyl)-*N,N′*-bis-(phenyl)benzidine (TPD), an emissive monolayer of colloidal QDs, a 27 nm thick hole blocking layer of 3,4,5-triphenyl-1,2,4-triazole (TAZ) (that limits exciton formation to near/at QD sites), a 20 nm thick electron transporting layer of tris(8-hydroxyquinoline) aluminum (Alq₃), and a 100 nm thick cathode of magnesium silver alloy, coated with a 20 nm thick silver protective layer (see Figure 1). We use three types of colloidaly synthesized QDs (see Supporting Information) to generate the red, green, and blue spectral components of the white LED. The red QD solution consisted of CdSe/ZnS core-shell QDs with a photoluminescence (PL) peak at wavelength $\lambda = 620$ nm. The green QD solution consisted of ZnSe/CdSe alloyed cores overcoated with a shell of ZnS with a PL peak at $\lambda = 540$ nm. Finally, the blue QD solution consisted of ZnCdS alloyed QDs with a PL peak at $\lambda = 440$ nm.

QD solutions for the white QD-LEDs were prepared by mixing red, green, and blue QD solutions so that the R:G:B QD ratio in the film is 1:2:10. The R:G:B QD ratio was chosen in part to compensate for the differences in PL efficiency of different QD samples. Additionally, QD-to-QD proximity in the electroluminescent QD monolayer enables exciton energy transfer from higher energy to lower energy QDs,[17,18] red shifting the overall emission, and necessitating a higher concentration of blue QDs in the QD monolayer. Consequently, blue QDs of high luminescence efficiency are needed for efficient QD-LED operation.

We found that CdSe/ZnS QDs emitting between 550 nm and 650 nm with a quantum yield (QY) of almost 90%[19] produced electroluminescence (EL) devices with external quantum efficiency (EQE) of ~2% in the orange and red.[5] These QDs readily accept excitons transferred from the blue- and green-emitting transport materials allowing the production of bright and efficient QD-LEDs. Core/shell/shell QDs made from ZnSe/CdSe/ZnS were produced with emission from 510 to 560 nm with a QY of ~70%,[20] enabling devices with EQE of 0.5%.[4] The lower EQE of these green devices is likely due to the greater difficulty of transferring excitons from the blue and green emitting transport materials to the QD monolayer, which does not absorb as strongly at those wavelengths as do redder QDs. Blue devices were initially constructed using CdS/ZnS particles, as in previously published devices;[6] however the QY of the QDs after

processing (15%) was not high enough to allow for efficient blue emission in the film. High QY ZnCdS alloyed QDs were then synthesized instead and found to emit between 400 and 500 nm with a QY of 40% after processing.[21] These materials were able to produce devices with greater EQE (0.35%) than previous devices and thus enabled the production of mixed films with an adequate blue QY to create reasonably efficient white EL devices. The EQE for the blue devices was still lower than for the green and red devices, mainly because resonant energy transfer of excitons from the organic transport materials is either less efficient, as in the case of TPD, or impossible, as in the case of Alq₃. In this case the device function is more dependent than the green or red devices on the ability of the transport materials to directly inject charge into the band structure of the QDs. Since it is more difficult to inject holes into the valence band of bluer QDs, these QDs tend to emit at higher voltages and as a result the white device CIE shifted to the blue with increased voltage.

EL spectra for the red, green, blue, and mixed-monolayer QD-LEDs are measured at near video brightness (Figure 2). The EL spectra of red and green QD-LEDs correspond to the color-saturated PL spectra characteristic of colloidal QDs, with CIE coordinates of (0.65, 0.34) and (0.31, 0.65), respectively. The blue QD-LED spectrum has a dominant QD component and weaker Alq₃ and TPD emission, consistent with energy transfer[22,23] and downconversion of the deep blue QD luminescence by Alq₃ (expected from the spectral overlap of Alq₃ absorption and blue QD PL). In contrast, spectral overlap of TPD PL and blue QD absorption is insufficient to provide complete quenching of TPD EL via energy transfer from TPD to blue QDs. CIE coordinates of the blue QD-LEDs are (0.19, 0.11). We note that the hole blocking TAZ layer should physically separate the blue QD monolayer Alq₃ film inhibiting QD-to-Alq₃ energy transfer and Alq₃ luminescence. However, the TAZ film is not planar when grown on the QD monolayer,[5,24] allowing pinholes to form in which some QDs come into contact with the Alq₃ film. This contributes to Alq₃ EL in blue QD-LEDs.

The emission spectrum of the mixed-monolayer QD-LED (Figure 2) shows a pronounced contribution of red, green, and blue QD EL components. The TPD EL signal is largely quenched due to efficient energy transfer to the red and green QDs. Alq₃ still appears to exhibit a weak spectral feature in
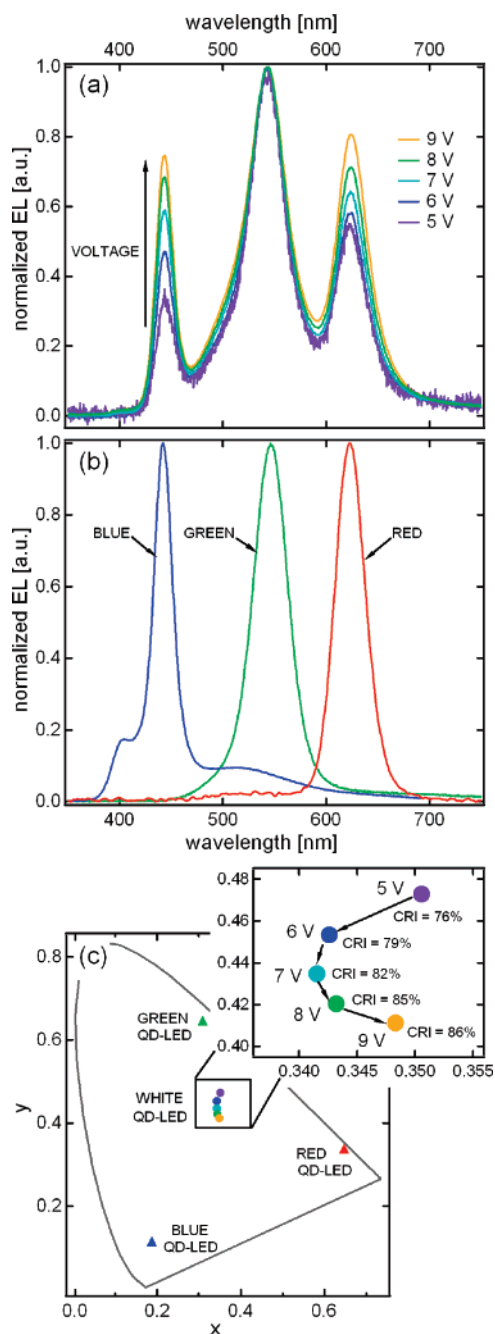

Figure 2. (a) Normalized EL spectra of a white QD-LED for a set of increasing applied voltages. The relative intensities of red and blue QD spectral components increase in comparison to the green QD component at higher biases. (b) Normalized EL spectra of red, green, and blue monochrome QD-LEDs (red, green, and blue lines, respectively). (c) CIE coordinates of the red, green, blue QD-LEDs (triangles). Circle symbols show the evolution of CIE coordinates and CRI of the white QD-LEDs upon increasing applied bias.

the white QD-LED spectrum analogous to the blue QD-LEDs. The mixed-monolayer QD-LED pixels appear uniformly luminescent, look "white" to the eye (Figure 1), with CIE coordinates (0.35, 0.41) at 9 V applied bias and color rendering index (CRI) of 86, when compared to 5500 K black body reference. Such high CRI compares favorably to conventional white light sources such as "cool white"
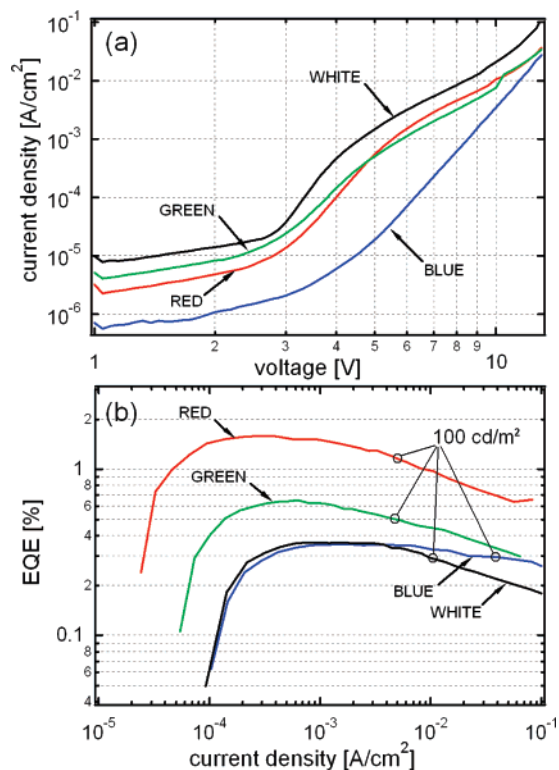

Figure 3. Current−voltage characteristics (a) and external electroluminescence quantum efficiency (b) measured for red, green, blue, and white QD-LEDs labeled with red, green, blue and black lines, respectively. The circled data points indicate device brightness of 100 cd/m^2.

fluorescent (CRI = 62), incandescent (CRI = 100), and dye-enhanced InGaN/GaN solid-state LEDs (CRI > 80).[25]

The peak EQE of our monochrome QD-LEDs are measured to be 1.6% at 4.6 V (0.29 mA/cm^2) for red devices, 0.65% at 5.2 V (0.63 mA/cm^2) for green, and 0.35% at 9.1 V for blue (1.73 mA/cm^2) (Figure 3). These values are consistent with previously reported QD-LEDs,[2−6] with our green and blue QD-LEDs more efficient than those in previous reports.[4,6] The peak EQE of white QD-LEDs is 0.36% at 5.0 V (1.51 mA/cm^2) (Figure 3), which corresponds to 0.9 cd/A and 0.57 lm/W, at a brightness of 13.5 cd/m^2. At 9 V applied bias, and optimal CIE position, the brightness was 92 cd/m^2, with efficiencies of 0.28% EQE, 0.7 cd/A, and 0.24 lm/W at 13 mA/cm^2 current. Maximum brightness topped 830 cd/m^2 at 14 V and 230 mA/cm^2.

The significant difference between EQEs of the red, green, and blue QD-LEDs originates from the difference in the QD band structures, which affect the two dominant QD excitation mechanisms in QD-LEDs:

(1) The QD energy band structure alignment with respect to the electron energy levels of neighboring TPD and TAZ layers determines the efficacy of electron and hole injection into the QD layer. From the bulk band structure and electron/hole masses of the QD materials, we expect that the energy barrier to hole injection increases for wider band gap QDs while an electron barrier is nonexistent in all of the structures (see the QD-LED energy band diagram in inset to Figure 4).
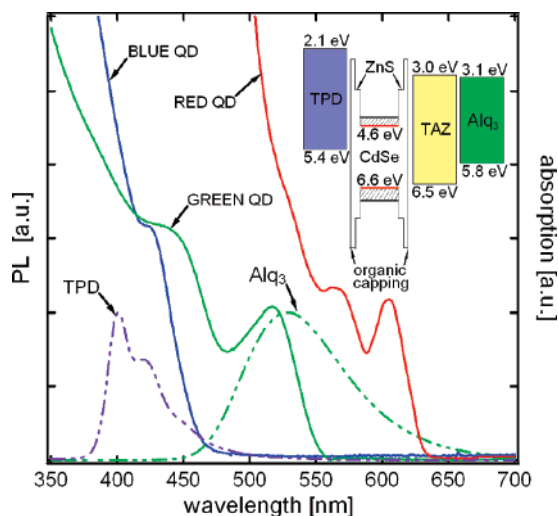
Figure 4. Red, green, and blue QD absorption spectra labeled with red, green, and blue solid lines, respectively, are shown together with TPD and Alq3 PL spectra labeled with purple and green dashed lines to demonstrate spectral overlaps. (inset) Suggested band diagram for the QD-LEDs of this study. Conduction and valence band position for the red QDs are labeled with red energy levels; the shaded area shows the range of likely energy level positions for the conduction and valence bands of the green and blue QDs.

(2) Resonant exciton energy transfer directs the excitons to the lowest available energy levels, favoring formation of the red excitons over the blue ones. For example, excitons formed on TPD in the vicinity of the QD layer resonantly transfer their energy to the QDs,[23] favoring energy transfer to red and green QDs over blue QDs due to the enhanced spectral overlap between TPD PL and QD absorption (see Figure 4). Also, with imperfections in the TAZ hole blocking layer, the Alq₃ film is in partial contact with the QDs and can either take energy from the more energetic blue QDs or transfer it back to red QDs.

In the red QD-LEDs, both direct charge injection and energy transfer from TPD and Alq₃ can contribute to the high EQEs of these devices. In the green QD-LEDs direct charge injection could be similar as for red QD-LEDs and energy transfer from the TPD to green QDs should be efficient due to the significant overlap of TPD emission and green QD absorption spectra and less efficient from Alq₃ to green QDs (Figure 4). The lower photoluminescence efficiency of the green QD solutions used in these experiments (~70%) as compared to the red QD solutions (90%) may also contribute to the lower EQE of green QD-LEDs (Figure 3).

The lower EQEs of the blue QD-LEDs (Figure 3) could be attributed to the low efficacy of hole injection from TPD into the blue QDs due to the increased potential barrier at this junction (see band lineup in inset to Figure 4) or to the reduced tunneling rate through the organic groups capping the blue QDs. The reduced hole injection is manifested as an increase in the turn-on voltage of blue QD-LEDs (Figure 3), leading to an excess electron charging of the QDs, which reduces the QD PL efficiency.[26] Additionally, energy transfer from the TPD film to blue QDs is not as efficient as that for red or green QDs (Figure 4), while at the same time blue

QDs can efficiently transfer their excitons to any Alq₃ molecules located within the Förster radius. The imperfections in the QD monolayer and TAZ film lead to charge transport directly through the organic layers and exciton formation within TPD and Alq₃ layers. In the case of green and red QDs, excitons formed in the organic layer can be resonantly transferred to QDs, but in the case of blue QDs these excitons radiatively recombine in the organic layer contributing to TPD and Alq₃ spectral features in the QD-LED EL spectra.

The mixed-monolayer QD-LEDs contain three types of QDs with different responses to charge injection, leading to a change in the EL spectrum at different driving conditions. Figure 2a shows the EL spectrum color shift in a mixed-monolayer QD-LED as the applied bias increases from 5 to 9 V, resulting in a small change of the CIE coordinates and CRI (see Figure 2c). With increasing voltage we observe an increase of the red and blue QD spectral components in the EL spectrum relative to the initially dominant green QD spectral component. This evolution of spectral features with increasing bias is consistent with the reduced efficacy of hole injection into blue QDs. At low applied bias (5 V) charge injection into the mixed QD film of the mixed-monolayer QD-LED is dominated by injection into the green and red QDs. Resonant energy transfer from green QDs to red QDs is inhibited by the relatively small number of both red and green QDs as compared to blue QDs in the mixed QD monolayer, so that the probability of locating a green QD next to a red QD is small. At higher applied biases charge injection into blue QDs becomes more efficient, and the EL component of the blue QDs becomes more significant. Increased exciton formation on blue QDs also benefits red and green QD luminescence due to exciton energy transfer from blue QDs to red and green QDs. Note that the energy transfer to red QDs is more efficient than that to green QDs due to an increased spectral overlap, with the consequence that with an increase of blue QD luminescence (at higher operating voltages), red QD luminescence rises more than the green QD luminescence. Exciton formation on the more numerous blue QDs governs the overall efficiency of white QD-LEDs which closely tracks the efficiency of the monochrome blue QD-LEDs (Figure 3).

The operation of the mixed-monolayer QD-LED is enabled by the use of identical electron transporting, hole blocking, and hole transporting layers in all of our monochrome QD-LEDs, which also imparts simplicity to color tuning the mixed-monolayer QD-LED sources. Colloidal QDs demonstrate exceptional PL stability exceeding 10⁹ turnovers in the most stable QD structures;[27] consequently concern over differential aging of different-color QD samples is minimal, assuring stability of spectral emission, as long as the remaining films that comprise the QD-LED stay unchanged.

Akin to mixing colors in a paint shop, the present work demonstrates that QD solutions can be precisely mixed to achieve a desired QD-LED spectrum at a desired driving condition.

its Shared Experimental Facilities, and the U.S. Army through the Institute for Soldier Nanotechnologies (DAAD-19-02-0002) and NIRT (subcontract GLV13-01).

Note Added after ASAP Publication. An incorrect version of Figure 3 appeared in the version published ASAP July 7, 2007; a corrected version was published ASAP July 19, 2007; affiliation line corrections were made in the version posted ASAP July 25, 2007.

Supporting Information Available: Experimental details including synthesis and device fabrication. This material is available free of charge via the Internet at http://pubs.acs.org.

References

(1) Murray, C. B.; Norris, D. J.; Bawendi, M. G. *J. Am. Chem. Soc.* **1993**, *115*, 8706−8715.
(2) Dabbousi, B. O.; Bawendi, M. G.; Onitsuka, O.; Rubner, M. F. *Appl. Phys. Lett.* **1995**, *66* (11), 1316−1318.
(3) Coe, S.; Woo, W.-K.; Bawendi, M. G.; Bulović, V. *Nature* **2002**, *420*, 800−803.
(4) Steckel, J. S.; Snee, P.; Coe-Sullivan, S.; Zimmer, J. P.; Halpert, J. E.; Anikeeva, P.; Kim, L.; Bulovic, V.; Bawendi, M. G. *Angew. Chem., Int. Ed.* **2006**, *45* (35), 5796−5799.
(5) Coe-Sullivan, S.; Steckel, J. S.; Woo, W.-K.; Bawendi, M. G.; Bulovic, V. *Adv. Funct. Mater.* **2005**, *15*, 1117−1124.
(6) Steckel, J. S.; Zimmer, J. P.; Coe-Sullivan, S.; Stott, N. E.; Bulović, V.; Bawendi, M. G. *Angew. Chem., Int. Ed.* **2004**, *43*, 2154−2158.
(7) Mueller, A. H.; Petruska, M. A.; Achermann, M.; Werder, D. J.; Akhadov, E. A.; Koleske, D. D.; Hoffbauer, M. A.; Klimov, V. I. *Nano Lett.* **2005**, *5*, 1039−1044.
(8) Caruge, J.-M.; Halpert, J. E.; Bulovic, V.; Bawendi, M. G. *Nano Lett.* **2006**, *6*, 2991−2994.
(9) Gao, M.; Richter, B.; Kirstein, S. *Adv. Mater.* **1997**, *9*, 802−805.
(10) Li, Y.; Rizzo, A.; Mazzeo, M.; Carbone, L.; Manna, L.; Cingolani, R.; Gigli, G. *J. Appl. Phys.* **2005**, *97*, 113501 1−4.
(11) Park, J. H.; Kim, J. Y.; Chin, B. D.; Kim, Y. C.; Kim, J. K.; Park O. O. *Nanotechnology* **2004**, *15*, 1217−1220.
(12) Lee, J.; Sundar, V. C.; Heine, J. R.; Bawendi, M. G.; Jensen, K. F. *Adv. Mater.* **2000**, *12*, 1102−1105.
(13) Bowers, M. J., II; McBride, J. R.; Rosenthal, S. J. *J. Am. Chem. Soc.* **2005**, *127*, 15378−15379.
(14) Chen, H. S.; Wang, S. J. J.; Lo, C. J.; Chi, J. Y. *Appl. Phys. Lett.* **2005**, *86*, 131905 1−3.
(15) Anikeeva, P. O.; Halpert, J. E.; Bawendi, M. G.; Bulović, V. Basic Research Needs for Solid-State Lighting, May 22−24, 2006.
(16) Li, Y.; Rizzo, A.; Cingolani, R.; Gigli, G. *Adv. Mater.* **2006**, *18*, 2545−2548.
(17) Kagan, C. R.; Murray, C. B.; Nirmal, M.; Bawendi, M. G. *Phys. Rev. Lett.* **1996**, *76*, 1517−1520.
(18) Crooker, S. A.; Hollingsworth, J. A.; Tretiak, S.; Klimov, V. I. *Phys. Rev. Lett.* **2002**, *89*, 186802 1−4.
(19) Hines, M. A.; Guyot-Sionnest, P. *J. Phys. Chem.* **1996**, *100*, 468−471.
(20) Ivanov, S. A.; Nanda, J.; Piryatinski, A.; Achermann, M.; Balet, L. P.; Bezel, I. V.; Anikeeva, P. O.; Tretiak, S.; Klimov, V. I. *J. Phys. Chem. B* **2004**, *108*, 10625−10630.
(21) Zhong, X.; Feng, Y.; Knoll, W.; Han, M. *J. Am. Chem. Soc.* **2003**, *125*, 13559−13563.
(22) Förster, Th. *Ann. Phys.* **1948**, *6*, 55−75.
(23) Kuhn, H. *J. Chem. Phys.* **1970**, *53*, 101−108.
(24) Huang, H.; Dorn, A.; Bulović, V.; Bawendi, M. G. *Appl. Phys. Lett.* **2007**, *90*, 023110 1−3.
(25) Krames, M. R.; Bhat, J.; Collins, D.; Gardner, N. F.; Gotz, W.; Lowery, C. H.; Ludowise, M.; Martin, P. S.; Mueller, G.; Mueller-Mach, R.; Rudaz, S.; Steigerwald, D. A.; Stockman, S. A.; Wierer J. J. *Phys. Status Solidi A* **2002**, *192*, 237−245.
(26) Neuhauser, R. G.; Shimizu, K. T.; Woo, W. K.; Empedocles, S. A.; Bawendi, M. G. *Phys. Rev. Lett.* **2000**, *85*, 3301−3304.
(27) Nirmal, M.; Dabousi, B. O.; Bawendi, M. G.; Macklin, J. J.; Trautman, J. K.; Harris, T. D.; Brus, L. E. *Nature* **1996**, *383*, 802−804.

NL0703424